



Azimuthally-differential pion femtoscopy relative to the third harmonic event plane in Pb–Pb collisions at $\sqrt{s_{NN}} = 2.76$ TeV

ALICE Collaboration*



ARTICLE INFO

Article history:

Received 5 April 2018

Received in revised form 18 June 2018

Accepted 19 June 2018

Available online 22 June 2018

Editor: L. Rolandi

ABSTRACT

Azimuthally-differential femtoscopy measurements, being sensitive to spatio-temporal characteristics of the source as well as to the collective velocity fields at freeze out, provide very important information on the nature and dynamics of the system evolution. While the HBT radii oscillations relative to the second harmonic event plane measured recently reflect mostly the spatial geometry of the source, model studies have shown that the HBT radii oscillations relative to the third harmonic event plane are predominantly defined by the velocity fields. In this Letter, we present the first results on azimuthally-differential pion femtoscopy relative to the third harmonic event plane as a function of the pion pair transverse momentum k_T for different collision centralities in Pb–Pb collisions at $\sqrt{s_{NN}} = 2.76$ TeV. We find that the R_{side} and R_{out} radii, which characterize the pion source size in the directions perpendicular and parallel to the pion transverse momentum, oscillate in phase relative to the third harmonic event plane, similar to the results from 3+1D hydrodynamical calculations. The observed radii oscillations unambiguously signal a collective expansion and anisotropy in the velocity fields. A comparison of the measured radii oscillations with the Blast-Wave model calculations indicate that the initial state triangularity is washed-out at freeze out.

© 2018 European Organization for Nuclear Research. Published by Elsevier B.V. This is an open access article under the CC BY license (<http://creativecommons.org/licenses/by/4.0/>). Funded by SCOAP³.

1. Introduction

Heavy-ion collisions at LHC energies create a hot and dense medium known as the quark–gluon plasma (QGP) [1]. The QGP fireball first expands, cools, and then freezes out into a collection of final-state hadrons. Correlations among the particles carry information about the space–time extent of the emitting source, and are imprinted on the final-state spectra due to a quantum-mechanical interference effect [2]. Commonly known as intensity or Hanbury–Brown–Twiss (HBT) interferometry, the correlation of two identical particles at small relative momentum, is an effective tool to study the space–time (“femtoscopic”) structure of the emitting source in relativistic heavy-ion collisions [3]. The initial state of a heavy-ion collision is characterized by spatial anisotropies that lead to anisotropies in pressure gradients, and consequently to azimuthal anisotropies in final particle distributions, commonly called anisotropic flow. Anisotropic flow is usually characterized by a Fourier decomposition of the particle azimuthal distribution and quantified by the flow coefficients v_n and the corresponding symmetry plane angles Ψ_n [4]. Elliptic flow is quantified by the second flow harmonic coefficient v_2 , whereas triangular flow [5] is quantified by v_3 . Due to the position–momentum correlations

in particle emission [6], the particles emitted at a particular angle relative to the flow plane carry information about the source as seen from that corresponding direction; these correlations also lead to the HBT radii to be sensitive to the collective velocity fields, from which information about the dynamics of the system evolution can be extracted.

Azimuthally-differential femtoscopy measurements can be performed relative to the direction of different harmonics event planes [7,8]. The measurements of the HBT radii with respect to the first harmonic event plane (directed flow) at the AGS [9] revealed that the source was tilted relative to the beam direction [10]. The HBT radii variations relative to the second harmonic event plane angle (Ψ_2) provide information on the pion source elliptic eccentricity at freeze-out. The recent ALICE measurements [11] indicate that due to the strong in-plane expansion the final-state source elliptic eccentricity is more than a factor 2–3 smaller compared to the initial-state. While the HBT radii modulations relative to Ψ_2 are defined mostly by the source geometry, the azimuthal dependence of the HBT radii relative to the third harmonic event plane (Ψ_3) originate predominantly in the anisotropies of the collective velocity fields – for a triangular, but static source the radii do not exhibit any oscillations [12]. Model studies [13,14] show that the anisotropy in expansion velocity as well as the system geometrical shape can be strongly constrained by azimuthally differential femtoscopy measurements relative to

* E-mail address: alice-publications@cern.ch.

Ψ_3 . The HBT radii oscillations relative to the third harmonic event plane have been first observed in Au–Au collisions at RHIC energy by the PHENIX Collaboration [15]. Unfortunately, due to large uncertainties these measurements did not allow to obtain detailed information on the origin of the observed oscillations.

In this Letter, the first azimuthally-differential femtoscopic measurement relative to the third harmonic event plane in Pb–Pb collisions at $\sqrt{s_{NN}} = 2.76$ TeV from the ALICE experiment are presented. We compare our results to the toy-model calculations from [13] to get an insight on the role of the anisotropies in the velocity fields and the system shape. In addition, we compare our results to a 3 + 1D hydrodynamical calculations [14] and a Blast-Wave Model [16] for a quantitative characterization of the final source shape.

2. Data analysis

The analysis was performed over the data sample recorded in 2011 during the second Pb–Pb running period at the LHC. Approximately 2 million minimum bias events, 29.2 million central trigger events, and 34.1 million semi-central trigger events were used. The minimum bias, semi-central, and central triggers used all require a signal in both V0 detectors [17]. The V0 detector, also used for the centrality determination [18], is a small angle detector of scintillator arrays covering pseudorapidity ranges $2.8 < \eta < 5.1$ and $-3.7 < \eta < -1.7$ for a collision vertex occurring at the center of the ALICE detector. The results of this analysis are reported for collision centrality classes expressed as ranges of the fraction of the inelastic Pb–Pb cross section: 0–5%, 5–10%, 10–20%, 20–30%, 30–40%, and 40–50%. Events with the primary event vertex along the beam direction $|V_z| < 8$ cm were used in this analysis to ensure a uniform pseudorapidity acceptance. A detailed description of the ALICE detector can be found in [19,20]. The Time Projection Chamber (TPC) has full azimuthal coverage and allows charged-particle track reconstruction in the pseudorapidity range $|\eta| < 0.8$, as well as particle identification via the specific ionization energy loss dE/dx associated with each track. In addition to the TPC, the Time-Of-Flight (TOF) detector was used for identification of particles with transverse momentum $p_T > 0.5$ GeV/c.

The TPC has 18 sectors covering full azimuth with 159 pad rows radially placed in each sector. Tracks with at least 80 space points in the TPC were used in this analysis. Tracks compatible with a decay in flight (kink topology) were rejected. The track quality was determined by the χ^2 of the Kalman filter fit to the reconstructed TPC clusters [21]. The χ^2 per degree of freedom was required to be less than 4. For primary track selection, only trajectories passing within 3.2 cm from the primary vertex in the longitudinal direction and 2.4 cm in the transverse direction were used. Based on the specific ionization energy loss in the TPC gas compared with the corresponding Bethe–Bloch curve, and the time of flight in TOF, a probability for each track to be a pion, kaon, proton, or electron was determined. Particles for which the pion probability was the largest were used in this analysis. This resulted in an overall purity above 95%, with small contamination from electrons in the region where the dE/dx for the two particle types overlap. Pions were selected in the pseudorapidity range $|\eta| < 0.8$ and $0.15 < p_T < 1.5$ GeV/c.

The correlation function $C(\mathbf{q})$ was calculated as

$$C(\mathbf{q}) = \frac{A(\mathbf{q})}{B(\mathbf{q})}, \quad (1)$$

where $\mathbf{q} = \mathbf{p}_1 - \mathbf{p}_2$ is the relative momentum of two pions, $A(\mathbf{q})$ is the distribution of particle pairs from the same event, and $B(\mathbf{q})$ is the background distribution of uncorrelated particle pairs. The

background distribution is built by using the mixed-event technique [22] in which pairs are made out of particles from three different events with similar centrality (less than 2% difference), event-plane angle (less than 6° difference), and event vertex position along the beam direction (less than 4 cm difference). Both the $A(\mathbf{q})$ and $B(\mathbf{q})$ distributions were measured differentially with respect to the third harmonic event-plane angle $\Psi_{EP,3}$. Note, that measurements relative to $\Psi_{EP,3}$ will smear any contribution from elliptic flow as the elliptic and triangular event planes are uncorrelated [23]. The third harmonic event-plane angle $\Psi_{EP,3}$ was determined using TPC tracks. To avoid auto-correlation each event was split into two subevents ($-0.8 < \eta < 0$ and $0 < \eta < 0.8$). Pairs were chosen from one subevent and the third harmonic event-plane angle $\Psi_{EP,3}$ was estimated using the particles from the other subevent, and vice-versa, with the event plane resolution determined from the correlations between the event planes determined in different subevents [4]. Requiring a minimum value in the two-track separation parameters $\Delta\varphi^* = |\varphi_1^* - \varphi_2^*|$ and $\Delta\eta = |\eta_1 - \eta_2|$ reduces two-track reconstruction effects such as track splitting or track merging. The quantity φ^* is defined in this analysis as the azimuthal angle of the track in the laboratory frame at the radial position of 1.6 m inside the TPC. Splitting is the effect when one track is reconstructed as two tracks, and merging is the effect of two tracks being reconstructed as one. Also, to reduce the splitting effect, pairs that share more than 5% of the TPC clusters were removed from the analysis. It is observed that at large relative momentum the correlation function is a constant, and the background pair distribution is normalized such that this constant is equal to unity. The analysis was performed for different collision centralities in several ranges of k_T , the magnitude of the pion-pair transverse momentum $\mathbf{k}_T = (\mathbf{p}_{T,1} + \mathbf{p}_{T,2})/2$, and in bins of $\Delta\varphi = \varphi_{\text{pair}} - \Psi_{EP,3}$, where φ_{pair} is the pair azimuthal angle. The Bertsch–Pratt [3,24] out-side–long coordinate system was used with the *long* direction pointing along the beam axis, *out* along the transverse pair momentum, and *side* being perpendicular to the other two. The three-dimensional correlation function was analyzed in the Longitudinally Co-Moving System (LCMS) [25], in which the total longitudinal momentum of the pair is zero, $p_{1,L} = -p_{2,L}$.

To isolate the Bose–Einstein contribution in the correlation function, effects due to final-state Coulomb repulsion must be taken into account. For that, the Bowler–Sinyukov fitting procedure [26,27] was used in which the Coulomb weight is only applied to the fraction of pairs (λ) that participate in the Bose–Einstein correlation. In this approach, the correlation function is fitted by

$$C(\mathbf{q}, \Delta\varphi) = N[(1 - \lambda) + \lambda K(\mathbf{q})(1 + G(\mathbf{q}, \Delta\varphi))], \quad (2)$$

where N is the normalization factor. The function $G(\mathbf{q}, \Delta\varphi)$ describes the Bose–Einstein correlations and $K(\mathbf{q})$ is the Coulomb part of the two-pion wave function integrated over a source function corresponding to $G(\mathbf{q})$. In this analysis the Gaussian form of $G(\mathbf{q}, \Delta\varphi)$ [28] was used

$$G(\mathbf{q}, \Delta\varphi) = \exp \left[-q_{\text{out}}^2 R_{\text{out}}^2(\Delta\varphi) - q_{\text{side}}^2 R_{\text{side}}^2(\Delta\varphi) - q_{\text{long}}^2 R_{\text{long}}^2(\Delta\varphi) - 2q_{\text{out}}q_{\text{side}}R_{\text{os}}^2(\Delta\varphi) - 2q_{\text{side}}q_{\text{long}}R_{\text{sl}}^2(\Delta\varphi) - 2q_{\text{out}}q_{\text{long}}R_{\text{ol}}^2(\Delta\varphi) \right], \quad (3)$$

where the parameters R_{out} , R_{side} , and R_{long} are traditionally called HBT radii in the *out*, *side*, and *long* directions. The cross-terms R_{os}^2 , R_{sl}^2 , and R_{ol}^2 describe the correlation in the *out-side*, *side-long*, and *out-long* directions, respectively.

The systematic uncertainties on the extracted radii, discussed below, vary in k_T and centrality. They include uncertainties related

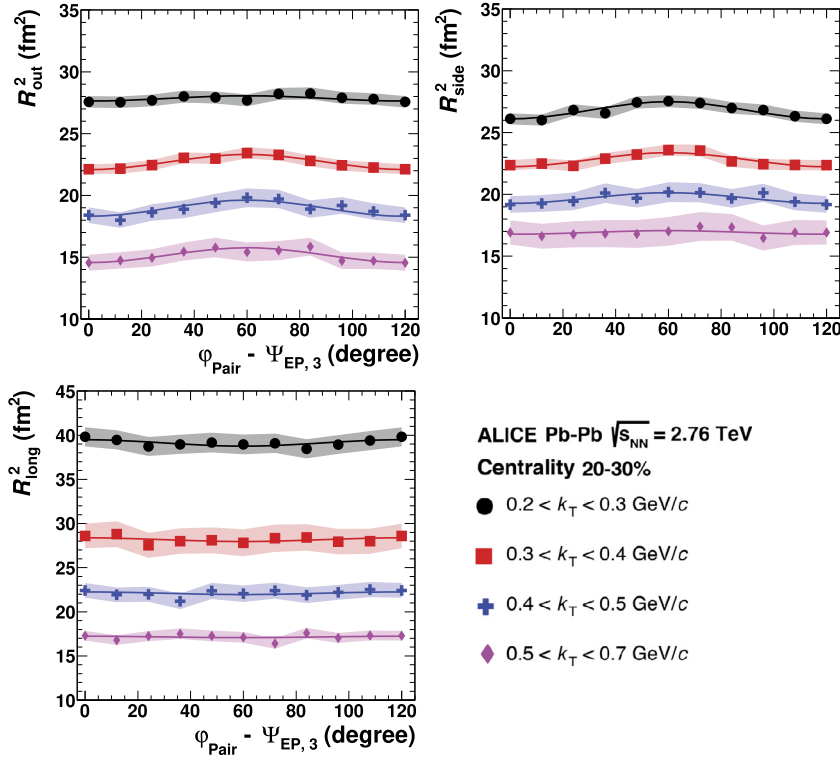


Fig. 1. The azimuthal dependence of R_{out}^2 , R_{side}^2 , and R_{long}^2 as a function of $\Delta\varphi = \varphi_{\text{pair}} - \Psi_3$ for centrality percentile 20–30% and four different k_T ranges. Solid lines represent the fit to the functional forms of Eq. (4). The shaded bands show the systematic uncertainty.

to the tracking efficiency and track quality, momentum resolution, different values for pair cuts ($\Delta\varphi^*$ and $\Delta\eta$), and correlation function fit ranges [29]. Similarly to the azimuthally inclusive analysis [29], different pair cuts were used, with the default values chosen based on a Monte Carlo study. The difference in the results from using different pair cuts rather than the default pair cuts were included in the systematic uncertainties (1–4%). For different k_T and centrality ranges, different fitting ranges of correlation function were used as the width of the correlation function depends on k_T and centrality range. The difference in the results from using different fit ranges are due to the contamination of electrons in the particle identification and the non-perfect Gaussian source (1–3%). We also studied the difference in the results by using positive and negative pion pairs separately as well as data obtained with two opposite magnetic field polarities of the ALICE L3 magnet. They have been analyzed separately and a small difference in the results (less than 3%) has been also accounted for in the systematic uncertainty. The total systematic uncertainties were obtained by adding in quadrature the contributions from all various sources mentioned above. The systematic uncertainty associated with the event plane determination is negligible compared to other systematic uncertainties; the procedure for the reaction plane resolution correction of the results is described in the next section.

3. Results

Fig. 1 presents the dependence of R_{out}^2 , R_{side}^2 , and R_{long}^2 on the pion emission angle relative to the third harmonic event plane for centrality 20–30% and different k_T ranges. Note that R_{out}^2 and R_{side}^2 exhibit in-phase oscillations (for a quantitative analysis, see below). Within the uncertainties of the measurement, R_{long}^2 oscillations, if any, are insignificant. Oscillations of R_{ol}^2 and R_{sl}^2 radii (not shown) are found to be consistent with zero, as expected due

to the source symmetry in longitudinal direction, and are not further investigated. The curves represent the fits to the data using the functions [12]:

$$\begin{aligned} R_{\mu}^2(\Delta\varphi) &= R_{\mu,0}^2 + 2R_{\mu,3}^2 \cos(3\Delta\varphi) \quad (\mu = \text{out, side, long}), \\ R_{\text{os}}^2(\Delta\varphi) &= R_{\text{os},0}^2 + 2R_{\text{os},3}^2 \sin(3\Delta\varphi). \end{aligned} \quad (4)$$

Fitting the radii's azimuthal dependence with the functional forms of Eq. (4) allows us to extract the average radii and the amplitudes of oscillations. The χ^2 per number of degree of freedom is 0.3–1.8 depending on k_T and centrality range. The results for the average radii $R_{\text{out},0}^2$, $R_{\text{side},0}^2$, and $R_{\text{os},0}^2$ were found to be consistent with those reported previously in [11] in azimuthally inclusive analysis. The extracted amplitudes of oscillations have to be corrected for the finite event plane resolution. There exist several methods for such a correction [30], which produce consistent results [31] well within uncertainties of this analysis. The results shown below have been obtained with the simplest method first used by the E895 Collaboration [9], in which the amplitude of oscillation is divided by the event plane resolution. In this analysis the event plane resolution correction factor is about 0.6–0.7, depending on centrality.

Fig. 2 shows the oscillation parameters $R_{\text{out},3}^2$, $R_{\text{side},3}^2$, $R_{\text{long},3}^2$, and $R_{\text{os},3}^2$ for different centrality and k_T ranges. All radii oscillations exhibit weak centrality dependence, likely reflecting the weak centrality dependence of the triangular flow itself. The k_T dependence is different for different radii oscillations: while the magnitudes of $R_{\text{out},3}^2$ and $R_{\text{os},3}^2$ are smallest for the smallest k_T range, it is opposite for $R_{\text{side},3}^2$ (and, possibly for $R_{\text{long},3}^2$), where the oscillations become stronger. The parameter $R_{\text{long},3}^2$ is consistent with zero within the systematic uncertainties while $R_{\text{os},3}^2$ is positive for all centralities and k_T ranges except for the lowest k_T range 0.2–0.3 GeV/c. Note that $R_{\text{out},3}^2$ and $R_{\text{side},3}^2$ are negative for

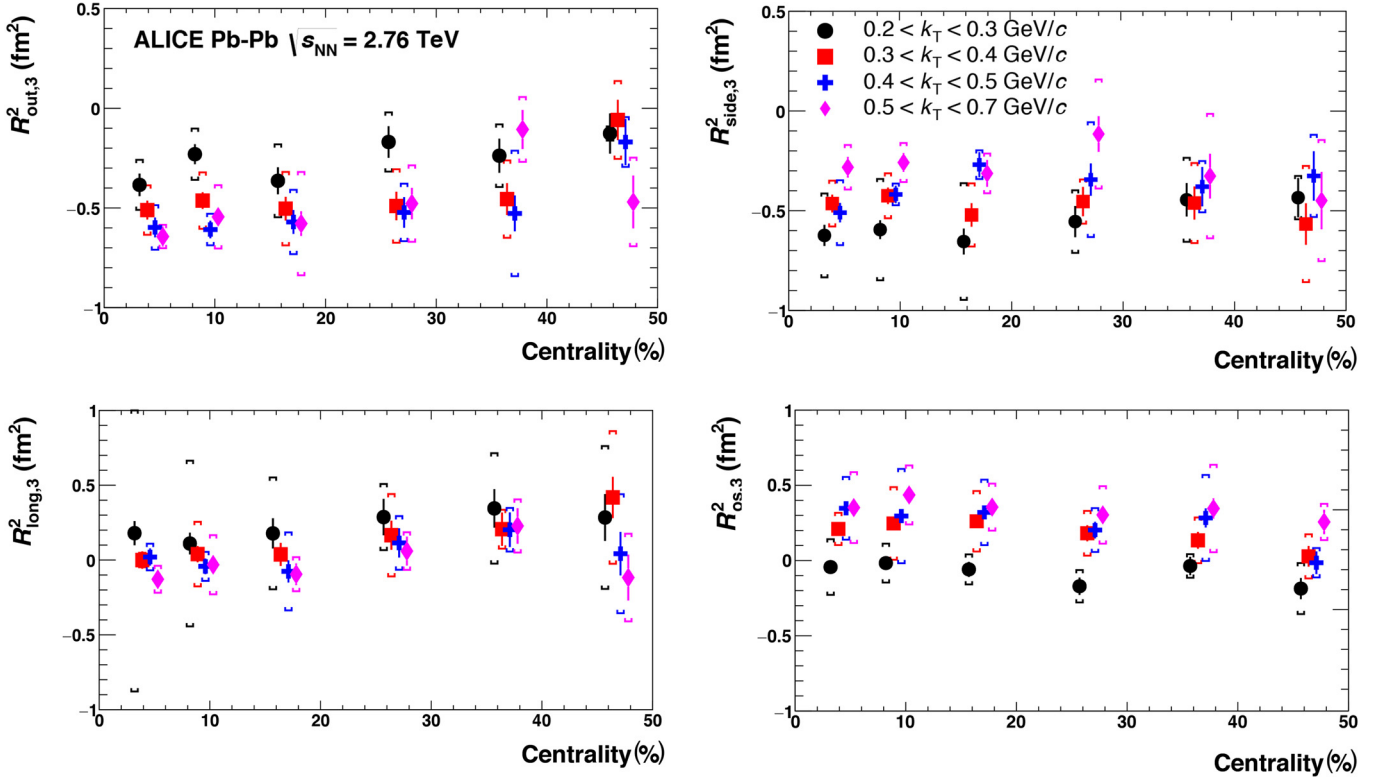


Fig. 2. The amplitudes of radii oscillations $R^2_{out,3}$, $R^2_{side,3}$, $R^2_{long,3}$, and $R^2_{os,3}$ versus centrality percentiles for four k_T ranges. Square brackets indicate systematic uncertainties.

all centralities and k_T ranges. In the toy model simulations [13] such phases of radii oscillations were observed only in the so-called “flow anisotropy dominated case” (a circular source with the radial expansion velocity including the third harmonic modulation) and not for “geometry dominated” case (triangular shape source with radial expansion velocity proportional to radial distance from the center, with corners having largest expansion velocity).

Fig. 3 shows the relative amplitudes of radius oscillations $R^2_{out,3}/R^2_{side,0}$, $R^2_{side,3}/R^2_{side,0}$, and $R^2_{os,3}/R^2_{side,0}$. Similar to the previous analyses and theoretical calculations [14] we report all the radii oscillations relative to the side radius the least affected by the emission time duration. There exist no obvious centrality dependence. As the average radii decrease with increasing k_T , the k_T dependence of relative oscillation amplitudes appear much stronger for “out” and “out-side” radii, while “side” radius relative amplitude exhibits no k_T dependence with the uncertainties. The shaded bands in Fig. 3 indicate the results of 3+1D hydrodynamical calculations [14]. These calculations assume constant shear viscosity to entropy ratio $\eta/s = 0.08$ and bulk viscosity that is nonzero in the hadronic phase $\zeta/s = 0.04$, and the initial density from a Glauber Monte Carlo model. The parameters of the model, were tuned to reproduce the measured charged particle spectra, the elliptic and triangular flow. We find that the relative amplitudes $R^2_{side,3}/R^2_{side,0}$ agree with these results rather well, while the relative amplitudes $R^2_{out,3}/R^2_{side,0}$ and $R^2_{os,2}/R^2_{side,0}$ agree only qualitatively. According to the 3+1D hydrodynamical calculations, the negative signs of $R^2_{side,3}$ and $R^2_{out,3}$ parameters are an indication that the initial triangularity has been washed-out or even reversed at freeze-out due to triangular flow [14].

To investigate further on the final source shape, we compare our results to the Blast-Wave model calculations [16]. In that model, the spatial geometry of the pion source at freeze-out is parameterized by

$$R(\phi) = R_0 \left(1 - \sum_{n=2}^{\infty} a_n \cos(n(\phi - \Psi_n)) \right), \quad (5)$$

where Ψ_n 's denote the orientations of the n -th order symmetry planes. The amplitudes a_n and the phases Ψ_n are model parameters. The magnitude of the transverse expansion velocity is parameterized as $v_t = \tanh \rho$, where the transverse rapidity ρ [13,16] is

$$\rho(\tilde{r}, \phi_b) = \rho_0 \tilde{r} \left(1 + \sum_{n=2}^{\infty} 2\rho_n \cos(n(\phi_b - \Psi_n)) \right). \quad (6)$$

Here $\tilde{r} = r/R(\phi)$, and $\phi_b(\phi)$ is the transverse boost direction assumed to be perpendicular to the surface of constant \tilde{r} . The results of this model presented below were obtained assuming a kinetic freeze-out temperature of 120 MeV, and maximum expansion rapidity $\rho_0 = 0.8$, tuned to describe single particle spectra. Fig. 4 shows the relative amplitudes of the radius oscillations $R^2_{out,3}/R^2_{out,0}$, and $R^2_{side,3}/R^2_{side,0}$ as a function of Blast-wave model third-order parameters, spatial anisotropy a_3 and transverse flow anisotropy ρ_3 . Thin dashed lines represent the lines of constant relative amplitudes, with numbers next to lines indicating the relative amplitude values. Thick dashed lines show the ALICE results for $R^2_{out,3}/R^2_{out,0}$ and $R^2_{side,3}/R^2_{side,0}$ with the thickness of the lines indicating the uncertainties. The intersection of the two dashed lines corresponds to a_3 and ρ_3 parameters consistent with ALICE measurements. The ALICE data and the Blast-Wave model calculations correspond to pairs with $k_T = 0.6$ GeV/c and the centrality range 5–10%. The comparison have been also performed for other centralities and the corresponding Blast-Wave model parameters have been deduced. Fig. 5 presents the final source spatial and transverse flow anisotropies for different centrality ranges from matching the ALICE data with the Blast-Wave model calculations. The contours correspond to one sigma uncertainty as derived from

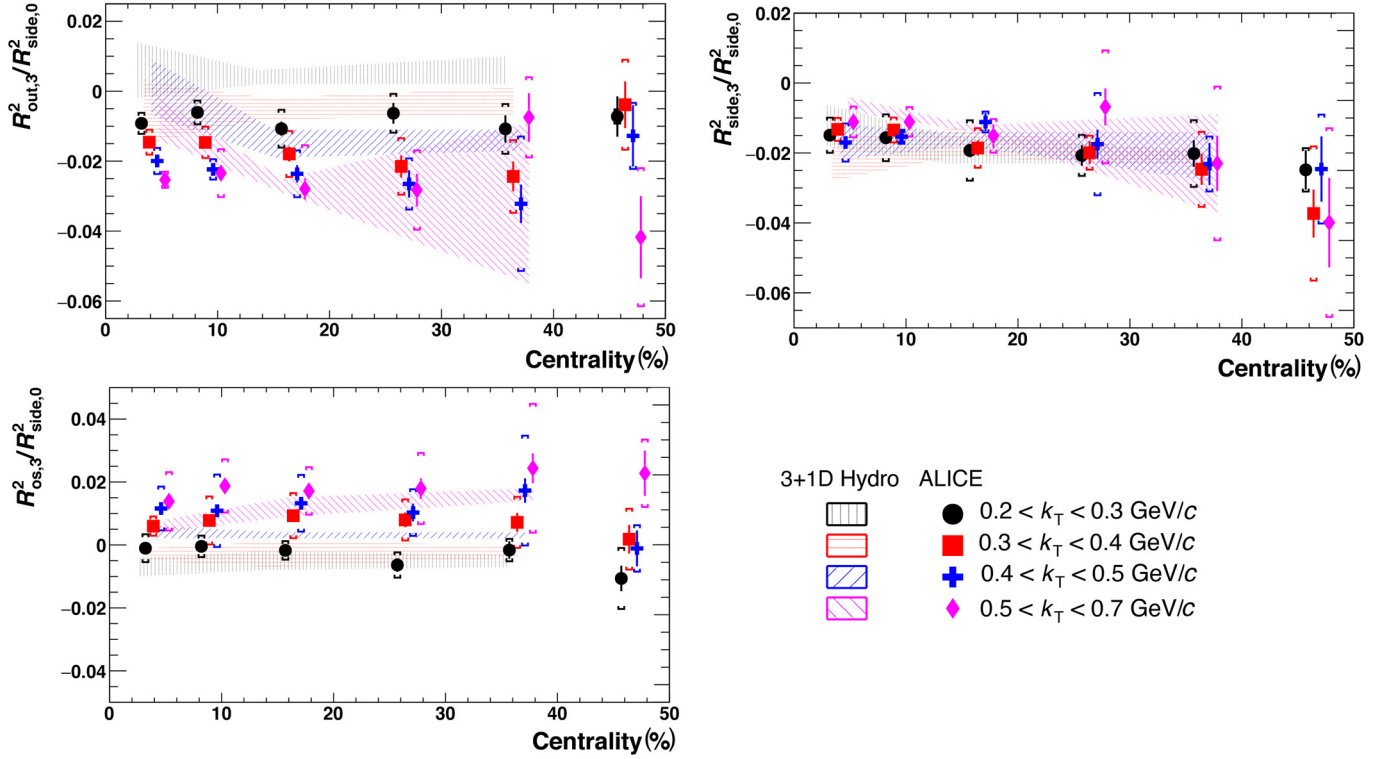


Fig. 3. Amplitudes of the relative radii oscillations $R_{out,3}^2/R_{side,0}^2$, $R_{side,3}^2/R_{side,0}^2$, and $R_{os,3}^2/R_{side,0}^2$ versus centrality for four k_T ranges. Square brackets indicate systematic uncertainties. The shaded bands are the 3+1D hydrodynamical calculations [14] and the width of the bands represent the uncertainties in the model calculations.

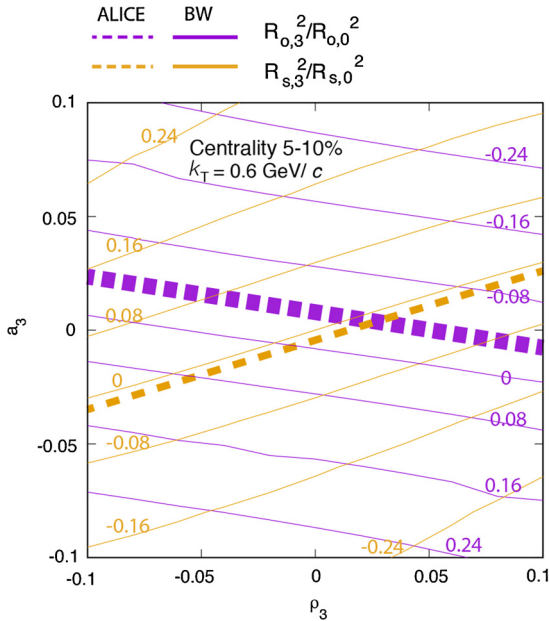


Fig. 4. The relative amplitudes of the radius oscillations $R_{out,3}^2/R_{out,0}^2$ and $R_{side,3}^2/R_{side,0}^2$ on the third-order anisotropies in space (a_3) and transverse flow (ρ_3) for the centrality range 5–10% and $k_T = 0.6$ GeV/c from the Blast-Wave model [16]. The thin dashed lines show the lines of a constant relative amplitude, in magenta for $R_{out,3}^2/R_{out,0}^2$ and in dark yellow for $R_{side,3}^2/R_{side,0}^2$. The thick lines show the corresponding ALICE results, with width of the lines representing the experimental uncertainties. (For interpretation of the colors in the figure(s), the reader is referred to the web version of this article.)

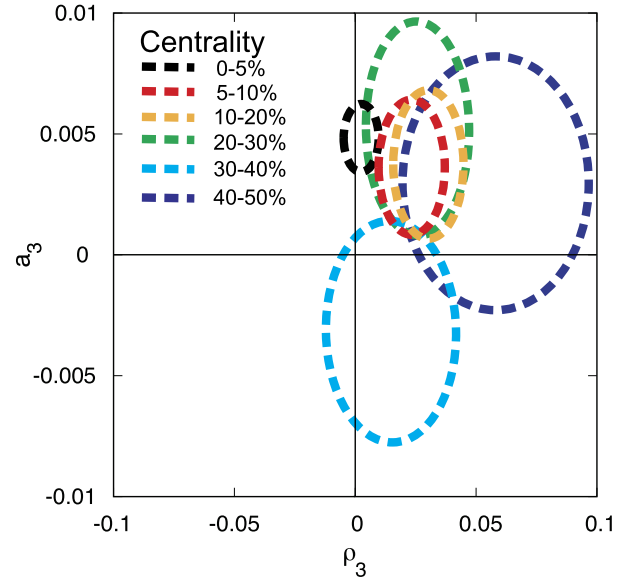


Fig. 5. Blast-Wave model [16] source parameters, final spatial (a_3) and transverse flow (ρ_3) anisotropies, for different centrality ranges, as obtained from the fit to ALICE radii oscillation parameters. The contours represent the one sigma uncertainty.

negative values of the final source anisotropy would be interpreted as that the triangular orientation at the initial-state is reversed at freeze out.

4. Summary

We have reported a measurement of two-pion azimuthally-differential femtoscopy relative to the third harmonic event plane in Pb–Pb collisions at $\sqrt{s_{NN}} = 2.76$ TeV. The observed oscillations

the fit of the model to the data. It is observed that the final source anisotropy is close to zero, significantly smaller than the initial triangular eccentricities that are typically of the order of 0.2–0.3. The

of the HBT radii unambiguously indicate a collective expansion of the system and anisotropy in collective velocity fields at freeze-out. Clear in-phase oscillations of R_{out} and R_{side} , with both $R_{\text{out},3}^2$ and $R_{\text{side},3}^2$ parameters (as defined in Eq. (4)) being negative, have been observed for all centralities and k_T ranges. According to model calculations [13] the observed R_{out} and R_{side} in-phase oscillations are characteristics of the source with strong triangular flow and close to zero spatial anisotropy. This conclusion is further confirmed by a detailed comparison of our results with the Blast-Wave model calculations [16], from which the parameters of the source, the spatial anisotropy and modulations in the radial expansion velocity, have been derived, with spatial triangular anisotropy being more than an order of magnitude smaller than the typical initial anisotropy values. The oscillation amplitudes exhibit weak centrality dependence, and in general decrease with decreasing k_T except for $R_{\text{side},3}^2$ which on opposite is the largest in the smallest k_T bin. The results of the 3+1D hydrodynamic calculations [14] are in a good qualitative agreement with our measurements but, quantitatively, the model predicts a stronger dependence of $R_{\text{out},3}^2$ oscillations on k_T than observed in the data.

Acknowledgements

We thank J. Cimerman and B. Tomasik for providing us with the results of the Blast-Model calculations [16].

The ALICE Collaboration would like to thank all its engineers and technicians for their invaluable contributions to the construction of the experiment and the CERN accelerator teams for the outstanding performance of the LHC complex. The ALICE Collaboration gratefully acknowledges the resources and support provided by all Grid centres and the Worldwide LHC Computing Grid (WLCG) collaboration. The ALICE Collaboration acknowledges the following funding agencies for their support in building and running the ALICE detector: A.I. Alikhanyan National Science Laboratory (Yerevan Physics Institute) Foundation (ANSL), State Committee of Science and World Federation of Scientists (WFS), Armenia; Austrian Academy of Sciences and Nationalstiftung für Forschung, Technologie und Entwicklung, Austria; Ministry of Communications and High Technologies, National Nuclear Research Center, Azerbaijan; Conselho Nacional de Desenvolvimento Científico e Tecnológico (CNPq), Universidade Federal do Rio Grande do Sul (UFRGS), Financiadora de Estudos e Projetos (Finep) and Fundação de Amparo à Pesquisa do Estado de São Paulo (FAPESP), Brazil; Ministry of Science & Technology of China (MSTC), National Natural Science Foundation of China (NSFC) and Ministry of Education of China (MOEC), China; Ministry of Science and Education, Croatia; Ministry of Education, Youth and Sports of the Czech Republic, Czech Republic; The Danish Council for Independent Research – Natural Sciences, the Carlsberg Foundation and Danish National Research Foundation (DNRF), Denmark; Helsinki Institute of Physics (HIP), Finland; Commissariat à l'Énergie Atomique (CEA) and Institut National de Physique Nucléaire et de Physique des Particules (IN2P3) and Centre National de la Recherche Scientifique (CNRS), France; Bundesministerium für Bildung, Wissenschaft, Forschung und Technologie (BMBF) and GSI Helmholtzzentrum für Schwerionenforschung GmbH, Germany; General Secretariat for Research and Technology, Ministry of Education, Research and Religions, Greece; National Research, Development and Innovation Office, Hungary; Department of Atomic Energy, Government of India (DAE), Department of Science and Technology, Government of India (DST), University Grants Commission, Government of India (UGC) and Council of Scientific and Industrial Research (CSIR), India; Indonesian Institute of Science, Indonesia; Centro Fermi – Museo Storico della Fisica e Centro Studi e Ricerche Enrico Fermi and Istituto Nazionale di Fisica Nucleare (INFN), Italy; Institute for Innova-

tive Science and Technology, Nagasaki Institute of Applied Science (IIST), Japan Society for the Promotion of Science (JSPS) KAKENHI and Japanese Ministry of Education, Culture, Sports, Science and Technology (MEXT), Japan; Consejo Nacional de Ciencia (CONACYT) y Tecnología, through Fondo de Cooperación Internacional en Ciencia y Tecnología (FONCICYT) and Dirección General de Asuntos del Personal Académico (DGAPA), Mexico; Nederlandse Organisatie voor Wetenschappelijk Onderzoek (NWO), Netherlands; The Research Council of Norway, Norway; Commission on Science and Technology for Sustainable Development in the South (COMSATS), Pakistan; Pontificia Universidad Católica del Perú, Peru; Ministry of Science and Higher Education and National Science Centre, Poland; Korea Institute of Science and Technology Information and National Research Foundation of Korea (NRF), Republic of Korea; Ministry of Education and Scientific Research, Institute of Atomic Physics and Romanian National Agency for Science, Technology and Innovation, Romania; Joint Institute for Nuclear Research (JINR), Ministry of Education and Science of the Russian Federation and National Research Centre Kurchatov Institute, Russia; Ministry of Education, Science, Research and Sport of the Slovak Republic, Slovakia; National Research Foundation of South Africa, South Africa; Centro de Aplicaciones Tecnológicas y Desarrollo Nuclear (CEADEN), Cubaenergía, Cuba and Centro de Investigaciones Energéticas, Medioambientales y Tecnológicas (CIEMAT), Spain; Swedish Research Council (VR) and Knut and Alice Wallenberg Foundation (KAW), Sweden; European Organization for Nuclear Research, Switzerland; National Science and Technology Development Agency (NSDTA), Suranaree University of Technology (SUT) and Office of the Higher Education Commission under NRU project of Thailand, Thailand; Turkish Atomic Energy Agency (TAEK), Turkey; National Academy of Sciences of Ukraine, Ukraine; Science and Technology Facilities Council (STFC), United Kingdom; National Science Foundation of the United States of America (NSF) and U.S. Department of Energy, Office of Nuclear Physics (DOE NP), United States of America.

References

- [1] B. Müller, J. Schukraft, B. Wyslouch, First results from Pb + Pb collisions at the LHC, *Annu. Rev. Nucl. Part. Sci.* 62 (2012) 361–386, arXiv:1202.3233 [hep-ex].
- [2] G. Goldhaber, S. Goldhaber, W. Lee, A. Pais, Influence of Bose–Einstein statistics on the anti-proton proton annihilation process, *Phys. Rev.* 120 (1960) 300–312.
- [3] G. Bertsch, M. Gong, M. Tohyama, Pion interferometry in ultrarelativistic heavy-ion collisions, *Phys. Rev. C* 37 (1988) 1896–1900.
- [4] A.M. Poskanzer, S.A. Voloshin, Methods for analyzing anisotropic flow in relativistic nuclear collisions, *Phys. Rev. C* 58 (1998) 1671–1678, arXiv:nucl-ex/9805001 [nucl-ex].
- [5] B. Alver, G. Roland, Collision geometry fluctuations and triangular flow in heavy-ion collisions, *Phys. Rev. C* 81 (2010) 054905, arXiv:1003.0194 [nucl-th], *Erratum: Phys. Rev. C* 82 (039903) (2010).
- [6] M.G. Bowler, Bose–Einstein symmetrization: coherence and chaos: with particular application to e^+e^- annihilation, *Z. Phys. C* 29 (1985) 617.
- [7] S.A. Voloshin, W.E. Cleland, HBT analysis of anisotropic transverse flow, *Phys. Rev. C* 53 (1996) 896–900, arXiv:nucl-th/9509025 [nucl-th].
- [8] S.A. Voloshin, W.E. Cleland, Anisotropic transverse flow and the HBT correlation function, *Phys. Rev. C* 54 (1996) 3212–3217, arXiv:nucl-th/9606033 [nucl-th].
- [9] E895 Collaboration, M.A. Lisa, et al., Azimuthal dependence of pion interferometry at the AGS, *Phys. Lett. B* 496 (2000) 1–8, arXiv:nucl-ex/0007022 [nucl-ex].
- [10] M.A. Lisa, U.W. Heinz, U.A. Wiedemann, Tilted pion sources from azimuthally sensitive HBT interferometry, *Phys. Lett. B* 489 (2000) 287–292, arXiv:nucl-th/0003022 [nucl-th].
- [11] ALICE Collaboration, D. Adamova, et al., Azimuthally differential pion femtoscopy in Pb–Pb collisions at $\sqrt{s_{NN}} = 2.76$ TeV, *Phys. Rev. Lett.* 118 (22) (2017) 222301, arXiv:1702.01612 [nucl-ex].
- [12] S.A. Voloshin, Femtoscopy of the system shape fluctuations in heavy ion collisions, *J. Phys. G* 38 (2011) 124097, arXiv:1106.5830 [nucl-th].
- [13] C.J. Plumberg, C. Shen, U.W. Heinz, Hanbury–Brown–Twiss interferometry relative to the triangular flow plane in heavy-ion collisions, *Phys. Rev. C* 88 (2013) 044914, arXiv:1306.1485 [nucl-th].
- [14] P. Bozek, Azimuthally sensitive femtoscopy in event-by-event hydrodynamics, *Phys. Rev. C* 89 (2014) 044904, arXiv:1401.4894 [nucl-th].

- [15] PHENIX Collaboration, A. Adare, et al., Azimuthal-angle dependence of charged-pion-interferometry measurements with respect to second- and third-order event planes in Au+Au collisions at $\sqrt{s_{NN}} = 200$ GeV, Phys. Rev. Lett. 112 (2014) 222301, arXiv:1401.7680 [nucl-ex].
- [16] J. Cimerman, B. Tomasik, M. Csanad, S. Lokos, Higher-order anisotropies in the Blast-Wave model – disentangling flow and density field anisotropies, Eur. Phys. J. A 53 (8) (2017) 161, arXiv:1702.01735 [nucl-th].
- [17] ALICE Collaboration, E. Abbas, et al., Performance of the ALICE VZERO system, JINST 8 (2013) P10016, arXiv:1306.3130 [nucl-ex].
- [18] ALICE Collaboration, K. Aamodt, et al., Centrality dependence of the charged-particle multiplicity density at mid-rapidity in Pb–Pb collisions at $\sqrt{s_{NN}} = 2.76$ TeV, Phys. Rev. Lett. 106 (2011) 032301, arXiv:1012.1657 [nucl-ex].
- [19] ALICE Collaboration, K. Aamodt, et al., The ALICE experiment at the CERN LHC, JINST 3 (2008) S08002.
- [20] ALICE Collaboration, B. Abelev, et al., Performance of the ALICE experiment at the CERN LHC, Int. J. Mod. Phys. A 29 (2014) 1430044, arXiv:1402.4476 [nucl-ex].
- [21] J. Alme, et al., The ALICE TPC, a large 3-dimensional tracking device with fast readout for ultra-high multiplicity events, Nucl. Instrum. Methods A 622 (2010) 316–367, arXiv:1001.1950 [physics.ins-det].
- [22] G. Kopylov, Like particle correlations as a tool to study the multiple production mechanism, Phys. Lett. B 50 (1974) 472–474.
- [23] ALICE Collaboration, K. Aamodt, et al., Higher harmonic anisotropic flow measurements of charged particles in Pb–Pb collisions at $\sqrt{s_{NN}} = 2.76$ TeV, Phys. Rev. Lett. 107 (2011) 032301, arXiv:1105.3865 [nucl-ex].
- [24] S. Pratt, Pion interferometry of quark–gluon plasma, Phys. Rev. D 33 (1986) 1314–1327.
- [25] S. Pratt, T. Csörgő, Structure of the peak in Bose–Einstein correlations, Conf. Proc. C 9106175 (1991) 75–90.
- [26] M.G. Bowler, Bose–Einstein correlations in quark initiated jets, Part. World 2 (1991) 1–6.
- [27] Y. Sinyukov, R. Lednicky, S. Akkelin, J. Pluta, B. Erasmus, Coulomb corrections for interferometry analysis of expanding hadron systems, Phys. Lett. B 432 (1998) 248–257.
- [28] S. Pratt, T. Csörgő, J. Zimányi, Detailed predictions for two-pion correlations in ultrarelativistic heavy-ion collisions, Phys. Rev. C 42 (Dec 1990) 2646–2652.
- [29] ALICE Collaboration, J. Adam, et al., Centrality dependence of pion freeze-out radii in Pb–Pb collisions at $\sqrt{s_{NN}} = 2.76$ TeV, Phys. Rev. C 93 (2016) 024905, arXiv:1507.06842 [nucl-ex].
- [30] M.A. Lisa, S. Pratt, R. Soltz, U. Wiedemann, Femtoscopy in relativistic heavy ion collisions, Annu. Rev. Nucl. Part. Sci. 55 (2005) 357–402, arXiv:nucl-ex/0505014 [nucl-ex].
- [31] STAR Collaboration, L. Adamczyk, et al., Beam-energy-dependent two-pion interferometry and the freeze-out eccentricity of pions measured in heavy ion collisions at the STAR detector, Phys. Rev. C 92 (2015) 014904, arXiv:1403.4972 [nucl-ex].

ALICE Collaboration

S. Acharya¹³⁹, F.T. Acosta²², D. Adamová⁹⁴, J. Adolfsson⁸¹, M.M. Aggarwal⁹⁸, G. Aglieri Rinella³⁶, M. Agnello³³, N. Agrawal⁴⁸, Z. Ahammed¹³⁹, S.U. Ahn⁷⁷, S. Aiola¹⁴⁴, A. Akindinov⁶⁴, M. Al-Turany¹⁰⁴, S.N. Alam¹³⁹, D.S.D. Albuquerque¹²⁰, D. Aleksandrov⁸⁸, B. Alessandro⁵⁸, R. Alfaro Molina⁷², Y. Ali¹⁶, A. Alici^{11,53,29}, A. Alkin³, J. Alme²⁴, T. Alt⁶⁹, L. Altenkamper²⁴, I. Altsybeev¹³⁸, C. Andrei⁴⁷, D. Andreou³⁶, H.A. Andrews¹⁰⁸, A. Andronic¹⁰⁴, M. Angeletti³⁶, V. Anguelov¹⁰², C. Anson¹⁷, T. Antičić¹⁰⁵, F. Antinori⁵⁶, P. Antonioli⁵³, N. Apadula⁸⁰, L. Aphecetche¹¹², H. Appelshäuser⁶⁹, S. Arcelli²⁹, R. Arnaldi⁵⁸, O.W. Arnold^{103,115}, I.C. Arsene²³, M. Arslandok¹⁰², B. Audurier¹¹², A. Augustinus³⁶, R. Averbeck¹⁰⁴, M.D. Azmi¹⁸, A. Badalà⁵⁵, Y.W. Baek^{60,76}, S. Bagnasco⁵⁸, R. Bailhache⁶⁹, R. Bala⁹⁹, A. Baldisseri¹³⁵, M. Ball⁴³, R.C. Baral⁸⁶, A.M. Barbano²⁸, R. Barbera³⁰, F. Barile⁵², L. Barioglio²⁸, G.G. Barnaföldi¹⁴³, L.S. Barnby⁹³, V. Barret¹³², P. Bartalini⁷, K. Barth³⁶, E. Bartsch⁶⁹, N. Bastid¹³², S. Basu¹⁴¹, G. Batigne¹¹², B. Batyunya⁷⁵, P.C. Batzing²³, J.L. Bazo Alba¹⁰⁹, I.G. Bearden⁸⁹, H. Beck¹⁰², C. Bedda⁶³, N.K. Behera⁶⁰, I. Belikov¹³⁴, F. Bellini^{36,29}, H. Bello Martinez², R. Bellwied¹²⁴, L.G.E. Beltran¹¹⁸, V. Belyaev⁹², G. Bencedi¹⁴³, S. Beole²⁸, A. Bercuci⁴⁷, Y. Berdnikov⁹⁶, D. Berenyi¹⁴³, R.A. Bertens¹²⁸, D. Berzano^{58,36}, L. Betev³⁶, P.P. Bhaduri¹³⁹, A. Bhasin⁹⁹, I.R. Bhat⁹⁹, B. Bhattacharjee⁴², J. Bhom¹¹⁶, A. Bianchi²⁸, L. Bianchi¹²⁴, N. Bianchi⁵¹, J. Bielčik³⁸, J. Bielčíková⁹⁴, A. Bilandzic^{103,115}, G. Biro¹⁴³, R. Biswas⁴, S. Biswas⁴, J.T. Blair¹¹⁷, D. Blau⁸⁸, C. Blume⁶⁹, G. Boca¹³⁶, F. Bock³⁶, A. Bogdanov⁹², L. Boldizsár¹⁴³, M. Bombara³⁹, G. Bonomi¹³⁷, M. Bonora³⁶, H. Borel¹³⁵, A. Borissov^{142,20}, M. Borri¹²⁶, E. Botta²⁸, C. Bourjau⁸⁹, L. Bratrud⁶⁹, P. Braun-Munzinger¹⁰⁴, M. Bregant¹¹⁹, T.A. Broker⁶⁹, M. Broz³⁸, E.J. Brucken⁴⁴, E. Bruna⁵⁸, G.E. Bruno^{36,35}, D. Budnikov¹⁰⁶, H. Buesching⁶⁹, S. Bufalino³³, P. Buhler¹¹¹, P. Buncic³⁶, O. Busch¹³¹, Z. Buthelezi⁷³, J.B. Butt¹⁶, J.T. Buxton¹⁹, J. Cabala¹¹⁴, D. Caffarri^{36,90}, H. Caines¹⁴⁴, A. Caliva¹⁰⁴, E. Calvo Villar¹⁰⁹, R.S. Camacho², P. Camerini²⁷, A.A. Capon¹¹¹, F. Carena³⁶, W. Carena³⁶, F. Carnesecchi^{11,29}, J. Castillo Castellanos¹³⁵, A.J. Castro¹²⁸, E.A.R. Casula⁵⁴, C. Ceballos Sanchez⁹, S. Chandra¹³⁹, B. Chang¹²⁵, W. Chang⁷, S. Chapeland³⁶, M. Chartier¹²⁶, S. Chattopadhyay¹³⁹, S. Chattopadhyay¹⁰⁷, A. Chauvin^{115,103}, C. Cheshkov¹³³, B. Cheynis¹³³, V. Chibante Barroso³⁶, D.D. Chinellato¹²⁰, S. Cho⁶⁰, P. Chochula³⁶, S. Choudhury¹³⁹, T. Chowdhury¹³², P. Christakoglou⁹⁰, C.H. Christensen⁸⁹, P. Christiansen⁸¹, T. Chujo¹³¹, S.U. Chung²⁰, C. Cicalo⁵⁴, L. Cifarelli^{11,29}, F. Cindolo⁵³, J. Cleymans¹²³, F. Colamaria^{52,35}, D. Colella^{36,52,65}, A. Collu⁸⁰, M. Colocci²⁹, M. Concas^{58,ii}, G. Conesa Balbastre⁷⁹, Z. Conesa del Valle⁶¹, J.G. Contreras³⁸, T.M. Cormier⁹⁵, Y. Corrales Morales⁵⁸, P. Cortese³⁴, M.R. Cosentino¹²¹, F. Costa³⁶, S. Costanza¹³⁶, J. Crkovská⁶¹, P. Crochet¹³², E. Cuautele⁷⁰, L. Cunqueiro^{95,142}, T. Dahms^{115,103}, A. Dainese⁵⁶, M.C. Danisch¹⁰², A. Danu⁶⁸, D. Das¹⁰⁷, I. Das¹⁰⁷, S. Das⁴, A. Dash⁸⁶, S. Dash⁴⁸, S. De⁴⁹, A. De Caro³², G. de Cataldo⁵², C. de Conti¹¹⁹, J. de Cuveland⁴⁰, A. De Falco²⁶, D. De Gruttola^{11,32}, N. De Marco⁵⁸, S. De Pasquale³², R.D. De Souza¹²⁰, H.F. Degenhardt¹¹⁹, A. Deisting^{104,102}, A. Deloff⁸⁵,

S. Delsanto²⁸, C. Deplano⁹⁰, P. Dhankeher⁴⁸, D. Di Bari³⁵, A. Di Mauro³⁶, B. Di Ruzza⁵⁶, R.A. Diaz⁹, T. Dietel¹²³, P. Dillenseger⁶⁹, Y. Ding⁷, R. Divià³⁶, Ø. Djuvsland²⁴, A. Dobrin³⁶, D. Domenicis Gimenez¹¹⁹, B. Dönigus⁶⁹, O. Dordic²³, L.V.R. Doremalen⁶³, A.K. Dubey¹³⁹, A. Dubla¹⁰⁴, L. Ducroux¹³³, S. Dudi⁹⁸, A.K. Duggal⁹⁸, M. Dukhishyam⁸⁶, P. Dupieux¹³², R.J. Ehlers¹⁴⁴, D. Elia⁵², E. Endress¹⁰⁹, H. Engel⁷⁴, E. Epple¹⁴⁴, B. Erasmus¹¹², F. Erhardt⁹⁷, M.R. Ersdal²⁴, B. Espagnon⁶¹, G. Eulisse³⁶, J. Eum²⁰, D. Evans¹⁰⁸, S. Evdokimov⁹¹, L. Fabbietti^{103,115}, M. Faggin³¹, J. Faivre⁷⁹, A. Fantoni⁵¹, M. Fasel⁹⁵, L. Feldkamp¹⁴², A. Feliciello⁵⁸, G. Feofilov¹³⁸, A. Fernández Téllez², A. Ferretti²⁸, A. Festanti^{31,36}, V.J.G. Feuillard^{135,132}, J. Figiel¹¹⁶, M.A.S. Figueredo¹¹⁹, S. Filchagin¹⁰⁶, D. Finogeev⁶², F.M. Fionda²⁴, M. Floris³⁶, S. Foertsch⁷³, P. Foka¹⁰⁴, S. Fokin⁸⁸, E. Fragiaco⁵⁹, A. Francescon³⁶, A. Francisco¹¹², U. Frankendorf¹⁰⁴, G.G. Fronze²⁸, U. Fuchs³⁶, C. Furget⁷⁹, A. Furs⁶², M. Fusco Girard³², J.J. Gaardhøje⁸⁹, M. Gagliardi²⁸, A.M. Gago¹⁰⁹, K. Gajdosova⁸⁹, M. Gallio²⁸, C.D. Galvan¹¹⁸, P. Ganoti⁸⁴, C. Garabatos¹⁰⁴, E. Garcia-Solis¹², K. Garg³⁰, C. Gargiulo³⁶, P. Gasik^{115,103}, E.F. Gauger¹¹⁷, M.B. Gay Ducati⁷¹, M. Germain¹¹², J. Ghosh¹⁰⁷, P. Ghosh¹³⁹, S.K. Ghosh⁴, P. Gianotti⁵¹, P. Giubellino^{104,58}, P. Giubilato³¹, P. Glässel¹⁰², D.M. Gómez Coral⁷², A. Gomez Ramirez⁷⁴, V. Gonzalez¹⁰⁴, P. González-Zamora², S. Gorbunov⁴⁰, L. Görlich¹¹⁶, S. Gotovac¹²⁷, V. Grabski⁷², L.K. Graczykowski¹⁴⁰, K.L. Graham¹⁰⁸, L. Greiner⁸⁰, A. Grelli⁶³, C. Grigoras³⁶, V. Grigoriev⁹², A. Grigoryan¹, S. Grigoryan⁷⁵, J.M. Gronefeld¹⁰⁴, F. Grosa³³, J.F. Grosse-Oetringhaus³⁶, R. Grosso¹⁰⁴, R. Guernane⁷⁹, B. Guerzoni²⁹, M. Guittiere¹¹², K. Gulbrandsen⁸⁹, T. Gunji¹³⁰, A. Gupta⁹⁹, R. Gupta⁹⁹, I.B. Guzman², R. Haake³⁶, M.K. Habib¹⁰⁴, C. Hadjidakis⁶¹, H. Hamagaki⁸², G. Hamar¹⁴³, J.C. Hamon¹³⁴, M.R. Haque⁶³, J.W. Harris¹⁴⁴, A. Harton¹², H. Hassan⁷⁹, D. Hatzifotiadou^{53,11}, S. Hayashi¹³⁰, S.T. Heckel⁶⁹, E. Hellbär⁶⁹, H. Helstrup³⁷, A. Herghelegiu⁴⁷, E.G. Hernandez², G. Herrera Corral¹⁰, F. Herrmann¹⁴², K.F. Hetland³⁷, T.E. Hilden⁴⁴, H. Hillemanns³⁶, C. Hills¹²⁶, B. Hippolyte¹³⁴, B. Hohlweger¹⁰³, D. Horak³⁸, S. Hornung¹⁰⁴, R. Hosokawa^{131,79}, P. Hristov³⁶, C. Hughes¹²⁸, P. Huhn⁶⁹, T.J. Humanic¹⁹, H. Hushnud¹⁰⁷, N. Hussain⁴², T. Hussain¹⁸, D. Hutter⁴⁰, D.S. Hwang²¹, J.P. Iddon¹²⁶, S.A. Iga Buitron⁷⁰, R. Ilkaev¹⁰⁶, M. Inaba¹³¹, M. Ippolitov⁸⁸, M.S. Islam¹⁰⁷, M. Ivanov¹⁰⁴, V. Ivanov⁹⁶, V. Izucheev⁹¹, B. Jacak⁸⁰, N. Jacazio²⁹, P.M. Jacobs⁸⁰, M.B. Jadhav⁴⁸, S. Jadlovská¹¹⁴, J. Jadlovsky¹¹⁴, S. Jaelani⁶³, C. Jahnke^{115,119}, M.J. Jakubowska¹⁴⁰, M.A. Janik¹⁴⁰, P.H.S.Y. Jayarathna¹²⁴, C. Jena⁸⁶, M. Jercic⁹⁷, R.T. Jimenez Bustamante¹⁰⁴, P.G. Jones¹⁰⁸, A. Jusko¹⁰⁸, P. Kalinak⁶⁵, A. Kalweit³⁶, J.H. Kang¹⁴⁵, V. Kaplin⁹², S. Kar^{139,7}, A. Karasu Uysal⁷⁸, O. Karavichev⁶², T. Karavicheva⁶², L. Karayan^{102,104}, P. Karczmarczyk³⁶, E. Karpechev⁶², U. Keschull⁷⁴, R. Keidel⁴⁶, D.L.D. Keijdener⁶³, M. Keil³⁶, B. Ketzer⁴³, Z. Khabanova⁹⁰, S. Khan¹⁸, S.A. Khan¹³⁹, A. Khanzadeev⁹⁶, Y. Kharlov⁹¹, A. Khatun¹⁸, A. Khuntia⁴⁹, M.M. Kielbowicz¹¹⁶, B. Kileng³⁷, B. Kim¹³¹, D. Kim¹⁴⁵, D.J. Kim¹²⁵, E.J. Kim¹⁴, H. Kim¹⁴⁵, J.S. Kim⁴¹, J. Kim¹⁰², M. Kim⁶⁰, S. Kim²¹, T. Kim¹⁴⁵, T. Kim¹⁴⁵, S. Kirsch⁴⁰, I. Kisel⁴⁰, S. Kiselev⁶⁴, A. Kisiel¹⁴⁰, G. Kiss¹⁴³, J.L. Klay⁶, C. Klein⁶⁹, J. Klein^{36,58}, C. Klein-Bösing¹⁴², S. Klewin¹⁰², A. Kluge³⁶, M.L. Knichel^{36,102}, A.G. Knospe¹²⁴, C. Kobdaj¹¹³, M. Kofarago¹⁴³, M.K. Köhler¹⁰², T. Kollegger¹⁰⁴, V. Kondratiev¹³⁸, N. Kondratyeva⁹², E. Kondratyuk⁹¹, A. Konevskikh⁶², M. Konyushikhin¹⁴¹, O. Kovalenko⁸⁵, V. Kovalenko¹³⁸, M. Kowalski¹¹⁶, I. Králik⁶⁵, A. Kravčáková³⁹, L. Kreis¹⁰⁴, M. Krivda^{108,65}, F. Krizek⁹⁴, M. Krüger⁶⁹, E. Kryshen⁹⁶, M. Krzewicki⁴⁰, A.M. Kubera¹⁹, V. Kučera^{60,94}, C. Kuhn¹³⁴, P.G. Kuijper⁹⁰, J. Kumar⁴⁸, L. Kumar⁹⁸, S. Kumar⁴⁸, S. Kundu⁸⁶, P. Kurashvili⁸⁵, A. Kurepin⁶², A.B. Kurepin⁶², A. Kuryakin¹⁰⁶, S. Kushpil⁹⁴, M.J. Kweon⁶⁰, Y. Kwon¹⁴⁵, S.L. La Pointe⁴⁰, P. La Rocca³⁰, C. Lagana Fernandes¹¹⁹, Y.S. Lai⁸⁰, I. Lakomov³⁶, R. Langoy¹²², K. Lapidus¹⁴⁴, C. Lara⁷⁴, A. Lardeux²³, P. Larionov⁵¹, A. Lattuca²⁸, E. Laudi³⁶, R. Lavicka³⁸, R. Lea²⁷, L. Leardini¹⁰², S. Lee¹⁴⁵, F. Lehas⁹⁰, S. Lehner¹¹¹, J. Lehrbach⁴⁰, R.C. Lemmon⁹³, E. Leogrande⁶³, I. León Monzón¹¹⁸, P. Lévai¹⁴³, X. Li¹³, X.L. Li⁷, J. Lien¹²², R. Lietava¹⁰⁸, B. Lim²⁰, S. Lindal²³, V. Lindenstruth⁴⁰, S.W. Lindsay¹²⁶, C. Lippmann¹⁰⁴, M.A. Lisa¹⁹, V. Litichevskiy⁴⁴, A. Liu⁸⁰, H.M. Ljunggren⁸¹, W.J. Llope¹⁴¹, D.F. Lodato⁶³, V. Loginov⁹², C. Loizides^{95,80}, P. Loncar¹²⁷, X. Lopez¹³², E. López Torres⁹, A. Lowe¹⁴³, P. Luettig⁶⁹, J.R. Luhder¹⁴², M. Lunardon³¹, G. Luparello⁵⁹, M. Lupi³⁶, A. Maevskaya⁶², M. Mager³⁶, S.M. Mahmood²³, A. Maire¹³⁴, R.D. Majka¹⁴⁴, M. Malaev⁹⁶, L. Malinina^{75,iii}, D. Mal'Kevich⁶⁴, P. Malzacher¹⁰⁴, A. Mamonov¹⁰⁶, V. Manko⁸⁸, F. Manso¹³², V. Manzari⁵², Y. Mao⁷, M. Marchisone^{129,73,133}, J. Mareš⁶⁷, G.V. Margagliotti²⁷, A. Margotti⁵³, J. Margutti⁶³, A. Marín¹⁰⁴, C. Markert¹¹⁷, M. Marquard⁶⁹, N.A. Martin¹⁰⁴, P. Martinengo³⁶, M.I. Martínez², G. Martínez García¹¹², M. Martinez Pedreira³⁶, S. Masciocchi¹⁰⁴, M. Maserà²⁸,

A. Masoni⁵⁴, L. Massacrier⁶¹, E. Masson¹¹², A. Mastroserio⁵², A.M. Mathis^{103,115}, P.F.T. Matuoka¹¹⁹,
 A. Matyja¹²⁸, C. Mayer¹¹⁶, M. Mazzilli³⁵, M.A. Mazzoni⁵⁷, F. Meddi²⁵, Y. Melikyan⁹²,
 A. Menchaca-Rocha⁷², J. Mercado Pérez¹⁰², M. Meres¹⁵, C.S. Meza¹⁰⁹, S. Mhlanga¹²³, Y. Miake¹³¹,
 L. Micheletti²⁸, M.M. Mieskolainen⁴⁴, D.L. Mihaylov¹⁰³, K. Mikhaylov^{64,75}, A. Mischke⁶³, A.N. Mishra⁷⁰,
 D. Miśkowiec¹⁰⁴, J. Mitra¹³⁹, C.M. Mitu⁶⁸, N. Mohammadi^{36,63}, A.P. Mohanty⁶³, B. Mohanty⁸⁶,
 M. Mohisin Khan^{18,iv}, D.A. Moreira De Godoy¹⁴², L.A.P. Moreno², S. Moretto³¹, A. Morreale¹¹²,
 A. Morsch³⁶, V. Muccifora⁵¹, E. Mudnic¹²⁷, D. Mühlheim¹⁴², S. Muhuri¹³⁹, M. Mukherjee⁴,
 J.D. Mulligan¹⁴⁴, M.G. Munhoz¹¹⁹, K. Munning⁴³, M.I.A. Munoz⁸⁰, R.H. Munzer⁶⁹, H. Murakami¹³⁰,
 S. Murray⁷³, L. Musa³⁶, J. Musinsky⁶⁵, C.J. Myers¹²⁴, J.W. Myrcha¹⁴⁰, B. Naik⁴⁸, R. Nair⁸⁵, B.K. Nandi⁴⁸,
 R. Nania^{53,11}, E. Nappi⁵², A. Narayan⁴⁸, M.U. Naru¹⁶, H. Natal da Luz¹¹⁹, C. Nattrass¹²⁸, S.R. Navarro²,
 K. Nayak⁸⁶, R. Nayak⁴⁸, T.K. Nayak¹³⁹, S. Nazarenko¹⁰⁶, R.A. Negrao De Oliveira^{69,36}, L. Nellen⁷⁰,
 S.V. Nesbo³⁷, G. Neskovic⁴⁰, F. Ng¹²⁴, M. Nicassio¹⁰⁴, J. Niedziela^{140,36}, B.S. Nielsen⁸⁹, S. Nikolaev⁸⁸,
 S. Nikulin⁸⁸, V. Nikulin⁹⁶, F. Noferini^{11,53}, P. Nomokonov⁷⁵, G. Nooren⁶³, J.C.C. Noris², J. Norman^{79,126},
 A. Nyanin⁸⁸, J. Nystrand²⁴, H. Oeschler^{20,102,i}, H. Oh¹⁴⁵, A. Ohlson¹⁰², L. Olah¹⁴³, J. Oleniacz¹⁴⁰,
 A.C. Oliveira Da Silva¹¹⁹, M.H. Oliver¹⁴⁴, J. Onderwaater¹⁰⁴, C. Oppedisano⁵⁸, R. Orava⁴⁴, M. Oravec¹¹⁴,
 A. Ortiz Velasquez⁷⁰, A. Oskarsson⁸¹, J. Otwinowski¹¹⁶, K. Oyama⁸², Y. Pachmayer¹⁰², V. Pacik⁸⁹,
 D. Pagano¹³⁷, G. Paić⁷⁰, P. Palni⁷, J. Pan¹⁴¹, A.K. Pandey⁴⁸, S. Panebianco¹³⁵, V. Papikyan¹, P. Pareek⁴⁹,
 J. Park⁶⁰, S. Parmar⁹⁸, A. Passfeld¹⁴², S.P. Pathak¹²⁴, R.N. Patra¹³⁹, B. Paul⁵⁸, H. Pei⁷, T. Peitzmann⁶³,
 X. Peng⁷, L.G. Pereira⁷¹, H. Pereira Da Costa¹³⁵, D. Peresunko^{92,88}, E. Perez Lezama⁶⁹, V. Peskov⁶⁹,
 Y. Pestov⁵, V. Petráček³⁸, M. Petrovici⁴⁷, C. Petta³⁰, R.P. Pezzi⁷¹, S. Piano⁵⁹, M. Pikna¹⁵, P. Pillot¹¹²,
 L.O.D.L. Pimentel⁸⁹, O. Pinazza^{53,36}, L. Pinsky¹²⁴, S. Pisano⁵¹, D.B. Piyarathna¹²⁴, M. Płoskoń⁸⁰,
 M. Planinic⁹⁷, F. Pliquett⁶⁹, J. Pluta¹⁴⁰, S. Pochybova¹⁴³, P.L.M. Podesta-Lerma¹¹⁸, M.G. Poghosyan⁹⁵,
 B. Polichtchouk⁹¹, N. Poljak⁹⁷, W. Poonsawat¹¹³, A. Pop⁴⁷, H. Poppenborg¹⁴²,
 S. Porteboeuf-Houssais¹³², V. Pozdniakov⁷⁵, S.K. Prasad⁴, R. Preghenella⁵³, F. Prino⁵⁸, C.A. Pruneau¹⁴¹,
 I. Pshenichnov⁶², M. Puccio²⁸, V. Punin¹⁰⁶, J. Putschke¹⁴¹, S. Raha⁴, S. Rajput⁹⁹, J. Rak¹²⁵,
 A. Rakotozafindrabe¹³⁵, L. Ramello³⁴, F. Rami¹³⁴, D.B. Rana¹²⁴, R. Raniwala¹⁰⁰, S. Raniwala¹⁰⁰,
 S.S. Räsänen⁴⁴, B.T. Rascanu⁶⁹, D. Rathee⁹⁸, V. Ratza⁴³, I. Ravasenga³³, K.F. Read^{128,95}, K. Redlich^{85,v},
 A. Rehman²⁴, P. Reichelt⁶⁹, F. Reidt³⁶, X. Ren⁷, R. Renfordt⁶⁹, A. Reshetin⁶², J.-P. Revol¹¹, K. Reygers¹⁰²,
 V. Riabov⁹⁶, T. Richert^{63,81}, M. Richter²³, P. Riedler³⁶, W. Riegler³⁶, F. Riggi³⁰, C. Ristea⁶⁸,
 M. Rodríguez Cahuantzi², K. Røed²³, R. Rogalev⁹¹, E. Rogochaya⁷⁵, D. Rohr³⁶, D. Röhrich²⁴,
 P.S. Rokita¹⁴⁰, F. Ronchetti⁵¹, E.D. Rosas⁷⁰, K. Roslon¹⁴⁰, P. Rosnet¹³², A. Rossi^{56,31}, A. Rotondi¹³⁶,
 F. Roukoutakis⁸⁴, C. Roy¹³⁴, P. Roy¹⁰⁷, O.V. Rueda⁷⁰, R. Rui²⁷, B. Rumyantsev⁷⁵, A. Rustamov⁸⁷,
 E. Ryabinkin⁸⁸, Y. Ryabov⁹⁶, A. Rybicki¹¹⁶, S. Saarinen⁴⁴, S. Sadhu¹³⁹, S. Sadovsky⁹¹, K. Šafařík³⁶,
 S.K. Saha¹³⁹, B. Sahoo⁴⁸, P. Sahoo⁴⁹, R. Sahoo⁴⁹, S. Sahoo⁶⁶, P.K. Sahu⁶⁶, J. Saini¹³⁹, S. Sakai¹³¹,
 M.A. Saleh¹⁴¹, S. Sambyal⁹⁹, V. Samsonov^{96,92}, A. Sandoval⁷², A. Sarkar⁷³, D. Sarkar¹³⁹, N. Sarkar¹³⁹,
 P. Sarma⁴², M.H.P. Sas⁶³, E. Scapparone⁵³, F. Scarlassara³¹, B. Schaefer⁹⁵, H.S. Scheid⁶⁹, C. Schiaua⁴⁷,
 R. Schicker¹⁰², C. Schmidt¹⁰⁴, H.R. Schmidt¹⁰¹, M.O. Schmidt¹⁰², M. Schmidt¹⁰¹, N.V. Schmidt^{95,69},
 J. Schukraft³⁶, Y. Schutz^{36,134}, K. Schwarz¹⁰⁴, K. Schweda¹⁰⁴, G. Scioli²⁹, E. Scomparin⁵⁸, M. Šeščík³⁹,
 J.E. Seger¹⁷, Y. Sekiguchi¹³⁰, D. Sekihata⁴⁵, I. Selyuzhenkov^{92,104}, K. Senosi⁷³, S. Senyukov¹³⁴,
 E. Serradilla⁷², P. Sett⁴⁸, A. Sevcenco⁶⁸, A. Shabanov⁶², A. Shabetai¹¹², R. Shahoyan³⁶, W. Shaikh¹⁰⁷,
 A. Shangaraev⁹¹, A. Sharma⁹⁸, A. Sharma⁹⁹, N. Sharma⁹⁸, A.I. Sheikh¹³⁹, K. Shigaki⁴⁵, M. Shimomura⁸³,
 S. Shirinkin⁶⁴, Q. Shou^{110,7}, K. Shtejer²⁸, Y. Sibiriak⁸⁸, S. Siddhanta⁵⁴, K.M. Sielewicz³⁶,
 T. Siemiarczuk⁸⁵, S. Silaeva⁸⁸, D. Silvermyr⁸¹, G. Simatovic⁹⁰, G. Simonetti^{36,103}, R. Singaraju¹³⁹,
 R. Singh⁸⁶, V. Singhal¹³⁹, T. Sinha¹⁰⁷, B. Sitar¹⁵, M. Sitta³⁴, T.B. Skaali²³, M. Slupecki¹²⁵, N. Smirnov¹⁴⁴,
 R.J.M. Snellings⁶³, T.W. Snellman¹²⁵, J. Song²⁰, F. Soramel³¹, S. Sorensen¹²⁸, F. Sozzi¹⁰⁴,
 I. Sputowska¹¹⁶, J. Stachel¹⁰², I. Stan⁶⁸, P. Stankus⁹⁵, E. Stenlund⁸¹, D. Stocco¹¹², M.M. Storetvedt³⁷,
 P. Strmen¹⁵, A.A.P. Suaide¹¹⁹, T. Sugitate⁴⁵, C. Suire⁶¹, M. Suleymanov¹⁶, M. Suljic^{36,27}, R. Sultanov⁶⁴,
 M. Šumbera⁹⁴, S. Sumowidagdo⁵⁰, K. Suzuki¹¹¹, S. Swain⁶⁶, A. Szabo¹⁵, I. Szarka¹⁵, U. Tabassam¹⁶,
 J. Takahashi¹²⁰, G.J. Tambave²⁴, N. Tanaka¹³¹, M. Tarhini^{61,112}, M. Tariq¹⁸, M.G. Tarzila⁴⁷, A. Tauro³⁶,
 G. Tejeda Muñoz², A. Telesca³⁶, C. Terrevoli³¹, B. Teyssier¹³³, D. Thakur⁴⁹, S. Thakur¹³⁹, D. Thomas¹¹⁷,
 F. Thoresen⁸⁹, R. Tieulent¹³³, A. Tikhonov⁶², A.R. Timmins¹²⁴, A. Toia⁶⁹, N. Topilskaya⁶², M. Toppi⁵¹,
 S.R. Torres¹¹⁸, S. Tripathy⁴⁹, S. Trogolo²⁸, G. Trombetta³⁵, L. Tropp³⁹, V. Trubnikov³, W.H. Trzaska¹²⁵,

T.P. Trzcinski¹⁴⁰, B.A. Trzeciak⁶³, T. Tsuji¹³⁰, A. Tumkin¹⁰⁶, R. Turrisi⁵⁶, T.S. Tveter²³, K. Ullaland²⁴, E.N. Umaka¹²⁴, A. Uras¹³³, G.L. Usai²⁶, A. Utrobicic⁹⁷, M. Vala¹¹⁴, J. Van Der Maarel⁶³, J.W. Van Hoorne³⁶, M. van Leeuwen⁶³, T. Vanat⁹⁴, P. Vande Vuyve³⁶, D. Varga¹⁴³, A. Vargas², M. Vargyas¹²⁵, R. Varma⁴⁸, M. Vasileiou⁸⁴, A. Vasiliev⁸⁸, A. Vauthier⁷⁹, O. Vázquez Doce^{115,103}, V. Vechernin¹³⁸, A.M. Veen⁶³, A. Velure²⁴, E. Vercellin²⁸, S. Vergara Limón², L. Vermunt⁶³, R. Vernet⁸, R. Vértési¹⁴³, L. Vickovic¹²⁷, J. Viinikainen¹²⁵, Z. Vilakazi¹²⁹, O. Villalobos Baillie¹⁰⁸, A. Villatoro Tello², A. Vinogradov⁸⁸, L. Vinogradov¹³⁸, T. Virgili³², V. Vislavicius⁸¹, A. Vodopyanov⁷⁵, M.A. Völkl¹⁰¹, K. Voloshin⁶⁴, S.A. Voloshin¹⁴¹, G. Volpe³⁵, B. von Haller³⁶, I. Vorobyev^{115,103}, D. Voscek¹¹⁴, D. Vranic^{36,104}, J. Vrláková³⁹, B. Wagner²⁴, H. Wang⁶³, M. Wang⁷, Y. Watanabe^{130,131}, M. Weber¹¹¹, S.G. Weber¹⁰⁴, A. Wegrzynek³⁶, D.F. Weiser¹⁰², S.C. Wenzel³⁶, J.P. Wessels¹⁴², U. Westerhoff¹⁴², A.M. Whitehead¹²³, J. Wiechula⁶⁹, J. Wikne²³, G. Wilk⁸⁵, J. Wilkinson⁵³, G.A. Willems^{36,142}, M.C.S. Williams⁵³, E. Willsher¹⁰⁸, B. Windelband¹⁰², W.E. Witt¹²⁸, R. Xu⁷, S. Yalcin⁷⁸, K. Yamakawa⁴⁵, P. Yang⁷, S. Yano⁴⁵, Z. Yin⁷, H. Yokoyama^{131,79}, I.-K. Yoo²⁰, J.H. Yoon⁶⁰, V. Yurchenko³, V. Zaccolo⁵⁸, A. Zaman¹⁶, C. Zampolli³⁶, H.J.C. Zanoli¹¹⁹, N. Zardoshti¹⁰⁸, A. Zarochentsev¹³⁸, P. Závada⁶⁷, N. Zaviyalov¹⁰⁶, H. Zbroszczyk¹⁴⁰, M. Zhalov⁹⁶, H. Zhang⁷, X. Zhang⁷, Y. Zhang⁷, Z. Zhang^{132,7}, C. Zhao²³, N. Zhigareva⁶⁴, D. Zhou⁷, Y. Zhou⁸⁹, Z. Zhou²⁴, H. Zhu⁷, J. Zhu⁷, Y. Zhu⁷, A. Zichichi^{29,11}, M.B. Zimmermann³⁶, G. Zinovjev³, J. Zmeskal¹¹¹, S. Zou⁷

¹ A.I. Alikhanyan National Science Laboratory (Yerevan Physics Institute) Foundation, Yerevan, Armenia

² Benemérita Universidad Autónoma de Puebla, Puebla, Mexico

³ Bogolyubov Institute for Theoretical Physics, National Academy of Sciences of Ukraine, Kiev, Ukraine

⁴ Bose Institute, Department of Physics and Centre for Astroparticle Physics and Space Science (CAPSS), Kolkata, India

⁵ Budker Institute for Nuclear Physics, Novosibirsk, Russia

⁶ California Polytechnic State University, San Luis Obispo, CA, United States

⁷ Central China Normal University, Wuhan, China

⁸ Centre de Calcul de l'IN2P3, Villeurbanne, Lyon, France

⁹ Centro de Aplicaciones Tecnológicas y Desarrollo Nuclear (CEADEN), Havana, Cuba

¹⁰ Centro de Investigación y de Estudios Avanzados (CINVESTAV), Mexico City and Mérida, Mexico

¹¹ Centro Fermi – Museo Storico della Fisica e Centro Studi e Ricerche "Enrico Fermi", Rome, Italy

¹² Chicago State University, Chicago, IL, United States

¹³ China Institute of Atomic Energy, Beijing, China

¹⁴ Chonbuk National University, Jeonju, Republic of Korea

¹⁵ Comenius University Bratislava, Faculty of Mathematics, Physics and Informatics, Bratislava, Slovakia

¹⁶ COMSATS Institute of Information Technology (CIIT), Islamabad, Pakistan

¹⁷ Creighton University, Omaha, NE, United States

¹⁸ Department of Physics, Aligarh Muslim University, Aligarh, India

¹⁹ Department of Physics, Ohio State University, Columbus, OH, United States

²⁰ Department of Physics, Pusan National University, Pusan, Republic of Korea

²¹ Department of Physics, Sejong University, Seoul, Republic of Korea

²² Department of Physics, University of California, Berkeley, CA, United States

²³ Department of Physics, University of Oslo, Oslo, Norway

²⁴ Department of Physics and Technology, University of Bergen, Bergen, Norway

²⁵ Dipartimento di Fisica dell'Università 'La Sapienza' and Sezione INFN, Rome, Italy

²⁶ Dipartimento di Fisica dell'Università and Sezione INFN, Cagliari, Italy

²⁷ Dipartimento di Fisica dell'Università and Sezione INFN, Trieste, Italy

²⁸ Dipartimento di Fisica dell'Università and Sezione INFN, Turin, Italy

²⁹ Dipartimento di Fisica e Astronomia dell'Università and Sezione INFN, Bologna, Italy

³⁰ Dipartimento di Fisica e Astronomia dell'Università and Sezione INFN, Catania, Italy

³¹ Dipartimento di Fisica e Astronomia dell'Università and Sezione INFN, Padova, Italy

³² Dipartimento di Fisica 'E.R. Caianiello' dell'Università and Gruppo Collegato INFN, Salerno, Italy

³³ Dipartimento DISAT del Politecnico and Sezione INFN, Turin, Italy

³⁴ Dipartimento di Scienze e Innovazione Tecnologica dell'Università del Piemonte Orientale and INFN Sezione di Torino, Alessandria, Italy

³⁵ Dipartimento Interateneo di Fisica 'M. Merlin' and Sezione INFN, Bari, Italy

³⁶ European Organization for Nuclear Research (CERN), Geneva, Switzerland

³⁷ Faculty of Engineering and Science, Western Norway University of Applied Sciences, Bergen, Norway

³⁸ Faculty of Nuclear Sciences and Physical Engineering, Czech Technical University in Prague, Prague, Czech Republic

³⁹ Faculty of Science, P.J. Šafárik University, Košice, Slovakia

⁴⁰ Frankfurt Institute for Advanced Studies, Johann Wolfgang Goethe-Universität Frankfurt, Frankfurt, Germany

⁴¹ Gangneung-Wonju National University, Gangneung, Republic of Korea

⁴² Gauhati University, Department of Physics, Guwahati, India

⁴³ Helmholtz-Institut für Strahlen- und Kernphysik, Rheinische Friedrich-Wilhelms-Universität Bonn, Bonn, Germany

⁴⁴ Helsinki Institute of Physics (HIP), Helsinki, Finland

⁴⁵ Hiroshima University, Hiroshima, Japan

⁴⁶ Hochschule Worms, Zentrum für Technologietransfer und Telekommunikation (ZIT), Worms, Germany

⁴⁷ Horia Hulubei National Institute of Physics and Nuclear Engineering, Bucharest, Romania

⁴⁸ Indian Institute of Technology Bombay (IIT), Mumbai, India

⁴⁹ Indian Institute of Technology Indore, Indore, India

⁵⁰ Indonesian Institute of Sciences, Jakarta, Indonesia

⁵¹ INFN, Laboratori Nazionali di Frascati, Frascati, Italy

⁵² INFN, Sezione di Bari, Bari, Italy

⁵³ INFN, Sezione di Bologna, Bologna, Italy

- 54 INFN, Sezione di Cagliari, Cagliari, Italy
- 55 INFN, Sezione di Catania, Catania, Italy
- 56 INFN, Sezione di Padova, Padova, Italy
- 57 INFN, Sezione di Roma, Rome, Italy
- 58 INFN, Sezione di Torino, Turin, Italy
- 59 INFN, Sezione di Trieste, Trieste, Italy
- 60 Inha University, Incheon, Republic of Korea
- 61 Institut de Physique Nucléaire d'Orsay (IPNO), Institut National de Physique Nucléaire et de Physique des Particules (IN2P3/CNRS), Université de Paris-Sud, Université Paris-Saclay, Orsay, France
- 62 Institute for Nuclear Research, Academy of Sciences, Moscow, Russia
- 63 Institute for Subatomic Physics, Utrecht University/Nikhef, Utrecht, Netherlands
- 64 Institute for Theoretical and Experimental Physics, Moscow, Russia
- 65 Institute of Experimental Physics, Slovak Academy of Sciences, Košice, Slovakia
- 66 Institute of Physics, Bhubaneswar, India
- 67 Institute of Physics of the Czech Academy of Sciences, Prague, Czech Republic
- 68 Institute of Space Science (ISS), Bucharest, Romania
- 69 Institut für Kernphysik, Johann Wolfgang Goethe-Universität Frankfurt, Frankfurt, Germany
- 70 Instituto de Ciencias Nucleares, Universidad Nacional Autónoma de México, Mexico City, Mexico
- 71 Instituto de Física, Universidade Federal do Rio Grande do Sul (UFRGS), Porto Alegre, Brazil
- 72 Instituto de Física, Universidad Nacional Autónoma de México, Mexico City, Mexico
- 73 iThemba LABS, National Research Foundation, Somerset West, South Africa
- 74 Johann-Wolfgang-Goethe Universität Frankfurt, Institut für Informatik, Fachbereich Informatik und Mathematik, Frankfurt, Germany
- 75 Joint Institute for Nuclear Research (JINR), Dubna, Russia
- 76 Konkuk University, Seoul, Republic of Korea
- 77 Korea Institute of Science and Technology Information, Daejeon, Republic of Korea
- 78 KTO Karatay University, Konya, Turkey
- 79 Laboratoire de Physique Subatomique et de Cosmologie, Université Grenoble-Alpes, CNRS-IN2P3, Grenoble, France
- 80 Lawrence Berkeley National Laboratory, Berkeley, CA, United States
- 81 Lund University, Department of Physics, Division of Particle Physics, Lund, Sweden
- 82 Nagasaki Institute of Applied Science, Nagasaki, Japan
- 83 Nara Women's University (NWU), Nara, Japan
- 84 National and Kapodistrian University of Athens, School of Science, Department of Physics, Athens, Greece
- 85 National Centre for Nuclear Research, Warsaw, Poland
- 86 National Institute of Science Education and Research, HBNI, Jatni, India
- 87 National Nuclear Research Center, Baku, Azerbaijan
- 88 National Research Centre Kurchatov Institute, Moscow, Russia
- 89 Niels Bohr Institute, University of Copenhagen, Copenhagen, Denmark
- 90 Nikhef, National Institute for Subatomic Physics, Amsterdam, Netherlands
- 91 NRC "Kurchatov Institute" IHEP, Protvino, Russia
- 92 NRNU Moscow Engineering Physics Institute, Moscow, Russia
- 93 Nuclear Physics Group, STFC Daresbury Laboratory, Daresbury, United Kingdom
- 94 Nuclear Physics Institute of the Czech Academy of Sciences, Řež u Prahy, Czech Republic
- 95 Oak Ridge National Laboratory, Oak Ridge, TN, United States
- 96 Petersburg Nuclear Physics Institute, Gatchina, Russia
- 97 Physics Department, Faculty of Science, University of Zagreb, Zagreb, Croatia
- 98 Physics Department, Panjab University, Chandigarh, India
- 99 Physics Department, University of Jammu, Jammu, India
- 100 Physics Department, University of Rajasthan, Jaipur, India
- 101 Physikalisches Institut, Eberhard-Karls-Universität Tübingen, Tübingen, Germany
- 102 Physikalisches Institut, Ruprecht-Karls-Universität Heidelberg, Heidelberg, Germany
- 103 Physik Department, Technische Universität München, Munich, Germany
- 104 Research Division and ExtreMe Matter Institute EMMI, GSI Helmholtzzentrum für Schwerionenforschung GmbH, Darmstadt, Germany
- 105 Rudjer Bošković Institute, Zagreb, Croatia
- 106 Russian Federal Nuclear Center (VNIIEF), Sarov, Russia
- 107 Saha Institute of Nuclear Physics, Kolkata, India
- 108 School of Physics and Astronomy, University of Birmingham, Birmingham, United Kingdom
- 109 Sección Física, Departamento de Ciencias, Pontificia Universidad Católica del Perú, Lima, Peru
- 110 Shanghai Institute of Applied Physics, Shanghai, China
- 111 Stefan Meyer Institut für Subatomare Physik (SMI), Vienna, Austria
- 112 SUBATECH, IMT Atlantique, Université de Nantes, CNRS-IN2P3, Nantes, France
- 113 Suranaree University of Technology, Nakhon Ratchasima, Thailand
- 114 Technical University of Košice, Košice, Slovakia
- 115 Technische Universität München, Excellence Cluster 'Universe', Munich, Germany
- 116 The Henryk Niewodniczanski Institute of Nuclear Physics, Polish Academy of Sciences, Cracow, Poland
- 117 The University of Texas at Austin, Austin, TX, United States
- 118 Universidad Autónoma de Sinaloa, Culiacán, Mexico
- 119 Universidade de São Paulo (USP), São Paulo, Brazil
- 120 Universidade Estadual de Campinas (UNICAMP), Campinas, Brazil
- 121 Universidade Federal do ABC, Santo Andre, Brazil
- 122 University College of Southeast Norway, Tonsberg, Norway
- 123 University of Cape Town, Cape Town, South Africa
- 124 University of Houston, Houston, TX, United States
- 125 University of Jyväskylä, Jyväskylä, Finland
- 126 University of Liverpool, Liverpool, United Kingdom
- 127 University of Split, Faculty of Electrical Engineering, Mechanical Engineering and Naval Architecture, Split, Croatia
- 128 University of Tennessee, Knoxville, TN, United States
- 129 University of the Witwatersrand, Johannesburg, South Africa
- 130 University of Tokyo, Tokyo, Japan
- 131 University of Tsukuba, Tsukuba, Japan

- ¹³² *Université Clermont Auvergne, CNRS/IN2P3, LPC, Clermont-Ferrand, France*
- ¹³³ *Université de Lyon, Université Lyon 1, CNRS/IN2P3, IPN-Lyon, Villeurbanne, Lyon, France*
- ¹³⁴ *Université de Strasbourg, CNRS, IPHC UMR 7178, F-67000 Strasbourg, France*
- ¹³⁵ *Université Paris-Saclay Centre d'Études de Saclay (CEA), IRFU, Department de Physique Nucléaire (DPhN), Saclay, France*
- ¹³⁶ *Università degli Studi di Pavia, Pavia, Italy*
- ¹³⁷ *Università di Brescia, Brescia, Italy*
- ¹³⁸ *V. Fock Institute for Physics, St. Petersburg State University, St. Petersburg, Russia*
- ¹³⁹ *Variable Energy Cyclotron Centre, Kolkata, India*
- ¹⁴⁰ *Warsaw University of Technology, Warsaw, Poland*
- ¹⁴¹ *Wayne State University, Detroit, MI, United States*
- ¹⁴² *Westfälische Wilhelms-Universität Münster, Institut für Kernphysik, Münster, Germany*
- ¹⁴³ *Wigner Research Centre for Physics, Hungarian Academy of Sciences, Budapest, Hungary*
- ¹⁴⁴ *Yale University, New Haven, CT, United States*
- ¹⁴⁵ *Yonsei University, Seoul, Republic of Korea*

ⁱ Deceased.

ⁱⁱ Dipartimento DET del Politecnico di Torino, Turin, Italy.

ⁱⁱⁱ M.V. Lomonosov Moscow State University, D.V. Skobeltsyn Institute of Nuclear, Physics, Moscow, Russia.

^{iv} Department of Applied Physics, Aligarh Muslim University, Aligarh, India.

^v Institute of Theoretical Physics, University of Wrocław, Poland.